Economic and environmental multi-optimal design and dispatch of solid oxide fuel cell based CCHP system

Rui Jing[a], Meng Wang[a], Wei Wang[a], Nigel Brandon[b], Ning Li[a], Jincan Chen[c], Yingru Zhao[a,*]

[a] *College of Energy, Xiamen University, Xiamen, China*
[b] *Earth Science and Engineering, Imperial College London, London, UK*
[c] *Department of Physics, Xiamen University, Xiamen, China*

Abstract

Combined cooling, heating and power system (CCHP) is an efficient alternative for building energy supply. Meanwhile, the advantages of high energy efficiency and low emission for solid oxide fuel cells (SOFCs) make the technology a promising prime mover for CCHP systems. In this study, a SOFC based CCHP system design and operation optimization model has been developed using the Mixed Integer Non-linear Programming (MINLP) approach. The model provides two capacity sizing options of the fixed size (user specified), and the optimal sizing. In the fixed size option, four dispatch strategies are considered, namely baseload, day/night, full-load, and electrical load following. In the optimal sizing option, the installed capacity of devices and the dispatch strategy are both optimized. Moreover, multi-objective optimizations are also conducted to optimize these two conflicting objectives simultaneously with the $\mathcal{E}$-constraint method. The optimal results are displayed by Pareto frontiers and the most desired solution points have been identified and verified by two decision-making approaches of LINMAP and TOPSIS. To make the model applicable to real world operation, novel constraints including part-load efficiency, equipment on/off, and numbers of start constraints are applied. Finally, the proposed model is applied to case study of a hospital in Shanghai, China considering state-of-the-art technical specifications, time-of-use energy pricing, and emission factors. The results indicate environmental advantages of SOFC based CCHP system. Moreover, the levelized cost of energy (LCOE) identified by the proposed optimal design and dispatch model would be 0.17 $/kWh, which is lower than the conventional energy system.

Keyword: SOFC-CCHP, optimal design and dispatch, MINLP model, multi-objective optimization, decision making, economic and environmental performance

---

* Corresponding author. Tel.: +86 592 5952781; Fax: +86 592 2188053.
E-mail address: yrzhao@xmu.edu.cn (Y. Zhao).

Nomenclature

Abbreviations

ATC	annual total cost
ACE	annual carbon emission
BL	baseload
CCHP	combined cooling heating and power
CRF	capital recovery factor
DG-BEAT	Distributed Generation Build Economic Assessment Tool
D/N	day/night
FL	full-load
FEL	following electrical load
HEX	heat exchanger
IEA	International Energy Agency
LINMAP	Linear Programming Technique for Multidimensional Analysis of Preference
LCOE	levelized cost of energy
MINLP	Mixed Integer Non-linear Programming
OPEX	operating expenditures
PEMFC	polymer electrolyte membrane fuel cell
SOFC	solid oxide fuel cell
TOPSIS	Technique for Order Preference by Similarity to an Ideal Solution

Symbols

C	cost ($)
CAP	installed capacity (kW)
E	electrical power (kW)
ED_{i+}	distance to ideal point
ED_{i-}	distance to non-ideal point
f	part load efficiency function
f_{ij}	location of each optimal point
f_j^{ideal}	location of ideal point
f_j^{nadir}	location of non-ideal point
PL	part load ratio
Q	thermal energy (kW)
Y_i	relative distance

Greek symbols

ω	heat-to-power ratio
η	nominal efficiency
α	modulation rate
δ	import/export status
β	on/off status
ϕ	heat charge/discharge status
φ	start limit variable
∂	emission factor
μ	energy conversion factor

Subscripts/superscript

fc	solid oxide fuel cell
s	season
h	hour
im	electricity import
ec	electrical chiller
re	heat recovered
b	boiler
st-in	heat storage charge
st-out	heat storage discharge
ac	absorption chiller
heat	heating energy
cool	cooling energy
NG	natural gas
LHV	low heating value
ex	electricity export
limit	installed capacity limit
st-init	initial state of heat storage
r	interest rate
t	each technology
n	project life
maint	maintenance cost
cap	capital cost

1. Introduction

Buildings including domestic and nondomestic buildings are gradually becoming the main contributor of global energy demand as estimated by the International Energy Agency (IEA) [1]. Considering an expected increase of population, along with the growing trend of urbanization and comfort level improvement, the energy demand in buildings will keep rising [2]. Combined cooling heating and power (CCHP) offers more efficient means to meet this increasing building energy demand [3]. By cascade utilization of the energy from fossil fuels or renewable energy sources, CCHP systems can improve energy efficiency and reduce environmental impact significantly [4]. Meanwhile, among all the available CCHP prime movers, fuel cells are considered as one of the most promising technologies [4, 5]. Compared to conventional combustion based engines, fuel cells have intrinsically better electrical efficiency (as high as 60%) with much lower pollutant emissions. In addition, fuel cells have no issues with noise or vibration, which make them easier to accommodate in buildings and further improves energy security [6].

1.1. Literature review

Among various fuel cell technologies, the Solid Oxide Fuel Cell (SOFC) is considered as a promising technology and is expected to play a key role in future distributed energy networks [7]. At the moment, the majority of research on CCHP systems focus on combustion based engines [2, 8-10], while the research on fuel cell systems focuses on thermodynamic modeling and optimization [11-15]. Less attention has been paid to the

system level study of fuel cell CCHP. Ranjbar et al. [16] established an evaluation model of a combined fuel cell and wind (hybrid CHP) power plant by evolutionary programming to assess the impact on performance and cost. Chen et al. [17] presented a hybrid CCHP system based on fuel cell and solar technology, and the system thermodynamic performance as well as the effects of key operating parameters have been discussed and analyzed. Wouters et al. [18] proposed a Mixed Integer Linear Programming (MILP) approach to optimize the design of a CCHP system to minimize the annualized cost of the system. Yang et al. [19] constructed a MILP model to optimally design district-scale distributed energy resource (DER) systems, and showed that the adoption of the proposed system could achieve significant economic benefits compared to conventional system. Sorace et al. [12] compared the low temperature polymer electrolyte membrane fuel cell (PEMFC) with SOFC as the prime mover of residential CHP systems from economic and environmental perspectives. The proposed system was connected to a heat pump and a domestic underfloor heating system. A sensitivity study was also undertaken to assess the impact of capital cost. The results indicate that a lower cost of energy was achieved by the SOFC due to its higher overall efficiency, however, the higher capital cost at the moment is still a barrier for diffusion of such systems. Fong et al. [20] proposed a fuel cell based CCHP system in an office building, and when operated at grid independent mode, the installed device capacity and the year round system performance were identified on monthly intervals. Pellegrino et al. [21] analyzed a fuel cell based micro CHP system in the European Union

residential sector by applying different operation strategies and further discussed the impact of various supporting schemes to promote the market entry of fuel cell technology. Facci et al. [22] designed and assessed solid oxide fuel cell based CCHP system applications in the residential sector. The optimally designed capacity was determined as a function of investment cost and control strategy, while a graph theory-based approach was applied to optimize the operation strategy. McLarty et al. [23] utilized a Distributed Generation Buildout Economic Assessment Tool (DG-BEAT) to analyze stationary fuel cell applications at several places in the U.S considering different conditions of energy prices, operation strategies, and complementary technologies. The results indicate that different operation strategies have significant impacts on project economy. Adam et al. [24] reviewed the fuel cell based micro-CHP system options for heat recovery. The grades of available heat from different fuel cell process units were discussed, and the integration of fuel cell based micro-CHP system with the building heating supply system was evaluated based on the match of temperature and cascade utilization of heat. Meanwhile, multi-objective optimization has been identified as a promising tool for system design.

1.2. Motivation

In this work, we present a data-driven MINLP model to tackle the optimal design and dispatch issue of an SOFC based CCHP system for project life of ten years. To model the SOFC based CCHP system more realistically, several constraints including part-load ratio, on/off limits, and device start limits have been applied. Meanwhile, multi-

objective optimizations have been conducted so as to evaluate the trade-off between cost and carbon emissions. Furthermore, this work provides both optimal and fixed sizing options as well as four types of pre-defined dispatch strategies. The proposed model has a high degree of freedom, and can be applied to specific projects by simply modifying the input parameters.

Compared to previous work, the major contributions of this study are as follows:

- Establish a MINLP optimal design and dispatch model for SOFC based CCHP system,
- Enable different sizing options and dispatch strategies, and compare the energy performance of each proposed option,
- Introduce the specified operation constraints of part-load ratio, on/off limits, and start-limits to make the model closer to practice,
- Implement the $\mathcal{E}$-constraint method to deal with the bi-objective optimization problem by generating a Pareto frontier of possible solutions,
- Apply two decision making approaches of LINMAP and TOPSIS to identify and verify the most desired solution from the Pareto frontier,
- Compare the levelized cost of energy (LCOE) of the proposed system with conventional energy systems, and quantify the economic and environmental benefits of fuel cell technology.

This paper is organized as follows. The problem is described in Section 2. Section

120 3 presents the fixed capacity option with certain defined operation strategies. The
121 optimal sizing and dispatch option is introduced in Section 4. Section 5 illustrates the
122 approach to conduct multi-objective optimization. A case study of the proposed model
123 is presented in Section 6. The results are discussed in Section 7, and conclusions made
124 in Section 8.

125

126 **2. Problem description**

127 In this study, the problem of SOFC based CCHP system design and dispatch
128 optimization with 10 years of project life has been tackled. The system is assumed to
129 have its own heating and cooling network, and a local micro electrical network but
130 available to import or export to the gird. The potential system components include: fuel
131 cell power generating unit, boiler, exhaust heat recovery unit, heat storage tank,
132 absorption chiller, and electrical chiller as presented in Fig. 1. The system design
133 optimization indicates that the technical combination as well as the corresponding
134 installed capacity of each selected component are optimized. And the system dispatch
135 optimization means the electrical/thermal power input and output of each system
136 component are optimized for each time step (1 hour in this study). In the proposed
137 system, the SOFC is fueled by pre-heated natural gas, whose composition is assumed
138 to be 80% CH_4, and 79% N_2 and 21% O_2 is assumed as the air composition [25, 26].
139 The compressed air with a compression ratio of 7, the SOFC stack temperature of 1073
140 K, the operating pressure of 709 kPa, and the fuel and oxidant utilization rate of 0.8 and

141 0.3 are also assumed respectively [27-29]. Reforming reactions are considered inside
142 the SOFC stack [30]. The product gas (1073 K) of the SOFC flows into an afterburner,
143 where the un-reacted fuel is burnt (1241 K). Upstream of the fuel cell, three heat
144 exchangers serve as pre-heaters, recovering heat from the exhaust gas of the afterburner
145 for preheating the inlet air, fuel and water. Then the residual heat of the exhaust gas (at
146 around 733 K) is further recovered to provide heating with heating supply header, or
147 provide cooling by incorporating with absorption chiller.

148 The building electrical, heating and cooling demand is fulfilled by the proposed fuel
149 cell based CCHP system. Thus, the overall problem can be stated as follows. Given,

150 - Electrical, heating and cooling demand of a building at certain time step (hourly),
151 - Technical parameters including 1) design energy conversion efficiency of each
152 device, 2) heat charge/discharge limit and efficiency for heat storage tank, 3) each
153 component's capacity limit,
154 - Economic parameters including capital and maintenance cost of each device,
155 - Emission rate of natural gas and purchased electricity,
156 - Time-of-use energy tariff including the purchased electricity, natural gas and
157 electricity feed-in,
158 - Project general information such as lifetime, interest rate.

159 Based on the given parameters, the outcomes include: 1) for both fixed and optimal
160 sizing options, the system energy, economic and environmental performance would be

evaluated, 2) for the fixed capacity option only, four dispatch strategies will be evaluated and optimized based on the objectives of minimizing annual total cost (ATC), annual carbon emission (ACE) or both; and 3) for optimal sizing option, the technology combination, installed capacity and dispatch strategy will be optimized based on single-objective and multi-objective optimizations. The overall flow chart of this study is illustrated in Fig. 2.

3. User specified design and dispatch

In this study, two sizing options are available which are the fixed sizing (user specified) option, and the optimal sizing option based on different objectives. In the fixed size option, the installed capacities of the SOFC and other major devices are defined before the optimization, with the value being large enough to cover all the energy demand of the building, thus the system performance is directly related to the dispatch strategy. Considering the features of the SOFC, four dispatch strategies are considered in this study namely baseload (BL) mode, day/night (D/N) mode, full-load (FL) mode, and following electrical load (FEL) mode, the description and rationale of these four dispatch strategies are presented in this section.

3.1. Baseload mode

In the baseload (BL) mode, the electrical output of a SOFC based CCHP system (E_{fc}) is assumed to meet the minimum electrical load of the building (E_{demand}) and keep constant, then the remaining electrical demand including the possible consumption by

182 the electrical chiller (E_{ec}) is met by purchased electricity from grid (E_{im}). This operation
183 strategy is relatively simple without selling electricity back to grid as derived in Eq. 1.
184 Meanwhile, the heating load is fulfilled by the recovered heat from power generation
185 (Q_{re}^{heat}), the natural gas boiler heat supply (Q_{b}^{heat}), and the possible interaction with a
186 storage tank by charging ($Q_{st\text{-}in}^{heat}$) and discharging heat energy ($Q_{st\text{-}out}^{heat}$). In addition,
187 cooling demand is satisfied by the electrical chiller (Q_{ec}^{cool}) and the absorption chiller
188 (Q_{ac}^{cool}) [31, 32]. This operation strategy is relatively simple without selling electricity
189 back to grid as derived in Eq. 2.

$$\begin{aligned} E_{fc,s,h} &= \min(E_{demand,s,h}) \ \forall s,h \\ E_{ec,s,h} + E_{demand,s,h} &= E_{fc,s,h} + E_{im,s,h} \ \forall s,h \end{aligned} \tag{1}$$

$$\begin{aligned} &Q_{re,s,h}^{heat} + Q_{b,s,h}^{heat} - Q_{st\text{-}in,s,h}^{heat} + Q_{st\text{-}out,s,h}^{heat} - Q_{ac,s,h}^{heat} \geq Q_{demand,s,h}^{heat} \ \forall s,h \\ &Q_{ec,s,h}^{cool} + Q_{ac,s,h}^{cool} \geq Q_{demand,s,h}^{cool} \ \forall s,h \end{aligned} \tag{2}$$

190 where h represents the time-step of one hour, and s means the seasons including winter,
191 summer and transition season.

192 In succession with Eq. 1 and 2, Eq. 3 defines the energy conversion rates of the
193 SOFC, where the ω represents the heat-to-power ratio of the SOFC. CAP_{fc} is the
194 installed capacity of the SOFC which is user pre-specified. β_{fc} is a binary variable to
195 control the on/off of the SOFC. PL_{fc} indicates the part-load ratio at each time step and
196 the part-load efficiency η_{fc} of the SOFC is assumed to vary with the part-load ratio
197 based on empirically fitted function with a high coefficient of correlation (R^2) value of
198 0.99 when the SOFC is not operating at full capacity [33]. Meanwhile, Q_{fc}^{NG} is the
199 natural gas energy consumed by the SOFC based on the low heating value (LHV) of

200 natural gas.

$$
\begin{aligned}
&Q_{\mathrm{re},s,h}^{\mathrm{heat}} = \omega \times E_{\mathrm{fc},s,h} \quad \forall s,h \\
&E_{\mathrm{fc},s,h} = \beta_{\mathrm{fc},s,h} \times PL_{\mathrm{fc},s,h} \times CAP_{\mathrm{fc}} \quad \forall s,h \\
&E_{\mathrm{fc},s,h} = \beta_{\mathrm{fc},s,h} \times \eta_{\mathrm{fc},s,h} \times Q_{\mathrm{fc},s,h}^{\mathrm{NG}} \quad \forall s,h \\
&\eta_{\mathrm{fc},s,h} = 0.494 \times (PL_{\mathrm{fc},s,h})^3 - 1.196 \times (PL_{\mathrm{fc},s,h})^2 + 0.945 \times PL_{\mathrm{fc},s,h} + 0.236
\end{aligned}
\tag{3}
$$

201 In addition, other devices' energy conversion rates have been given in Eq. 4, where
202 the rated efficiency of electrical chiller, absorption chiller and boiler are provided in
203 Table 2 [3, 22, 34]. and the COP of absorption chiller (η_{ac}) under non-standard
204 conditions has been empirically fitted [35].

$$
\begin{aligned}
&Q_{\mathrm{ac},s,h}^{\mathrm{cool}} = \beta_{\mathrm{ac},s,h} \times \eta_{\mathrm{ac},s,h} \times Q_{\mathrm{ac},s,h}^{\mathrm{heat}} \quad \forall s,h \\
&\eta_{\mathrm{ac},s,h} = 0.0001 \times (PL_{\mathrm{ac,s,h}})^3 - 0.0061 \times (PL_{\mathrm{ac,s,h}})^2 + 0.0578 \times PL_{\mathrm{ac,s,h}} + 0.8114 \\
&Q_{\mathrm{ec},s,h}^{\mathrm{cool}} = \beta_{\mathrm{ec},s,h} \times \eta_{\mathrm{ec}} \times E_{\mathrm{ec},s,h} \quad \forall s,h \\
&Q_{\mathrm{b},s,h}^{\mathrm{heat}} = \beta_{\mathrm{b},s,h} \times \eta_{\mathrm{b}} \times Q_{\mathrm{b},s,h}^{\mathrm{NG}} \quad \forall s,h
\end{aligned}
\tag{4}
$$

205 **3.2. Day/night mode**

206 In the day/night (D/N) mode, the SOFC based CCHP system output is modulated at a
207 certain rate and stays constant during each time slot of a day [32]. A modulation rate of
208 50% is applied at night (22:00 to 8:00 next day), while during the day-time period (8:00
209 to 22:00), the system is operated at full capacity (installed capacity). The electrical
210 constraints are shown in Eq. 5, while the heating, cooling and other constraints are
211 similar to baseload mode as shown in Eq. 2-4.

$$
\begin{aligned}
&\text{Peak period: } E_{\mathrm{fc},s,h} = \alpha_1 \times CAP_{\mathrm{fc}} \quad h = h_9 \sim h_{20} \text{ and } \alpha_1 = 100\% \ \forall s \\
&\quad \text{If } E_{\mathrm{demand},s,h} + E_{\mathrm{ec},s,h} \le E_{\mathrm{fc},s,h} \Rightarrow E_{\mathrm{ex},s,h} = E_{\mathrm{fc},s,h} - E_{\mathrm{demand},s,h} - E_{\mathrm{ec},s,h} \quad \forall s \\
&\quad \text{Else } E_{\mathrm{im},s,h} = E_{\mathrm{demand},s,h} + E_{\mathrm{ec},s,h} - E_{\mathrm{fc},s,h} \quad \forall s \\
&\text{Off-peak period: } E_{\mathrm{fc},s,h} = \alpha_2 \times CAP_{\mathrm{fc}} \quad h = h_0 \sim h_8 \ \cap \ h_{21} \sim h_{23} \text{ and } \alpha_2 = 50\% \ \forall s \\
&\quad \text{If } E_{\mathrm{demand},s,h} + E_{\mathrm{ec},s,h} \le E_{\mathrm{fc},s,h} \Rightarrow E_{\mathrm{ex},s,h} = E_{\mathrm{fc},s,h} - E_{\mathrm{demand},s,h} - E_{\mathrm{ec},s,h} \quad \forall s \\
&\quad \text{Else } E_{\mathrm{im},s,h} = E_{\mathrm{demand},s,h} + E_{\mathrm{ec},s,h} - E_{\mathrm{fc},s,h} \quad \forall s
\end{aligned}
\tag{5}
$$

212 **3.3. Full-load mode**

Full load (FL) mode indicates that the SOFC based CCHP system is operated at full capacity, which means the SOFC's output is constantly at installed capacity all day. The system is assumed to interact with the gird if the generated electricity is surplus or insufficient to meet the electrical demand, meanwhile the boiler, the absorption chiller, and the electrical chiller will be adopted if needed [7]. The electrical demand is met based on the following equations. Meanwhile, the heating, cooling and other constraints are similar to the baseload mode.

$$\begin{aligned} &E_{\mathrm{fc},s,h} = 100\% \times CAP_{\mathrm{fc}} \ \forall s,h \\ &\text{If } E_{\mathrm{fc},s,h} \geq E_{\mathrm{demand},s,h} + E_{\mathrm{ec},s,h} \Rightarrow E_{\mathrm{ex},s,h} = E_{\mathrm{fc},s,h} - E_{\mathrm{demand},s,h} - E_{\mathrm{ec},s,h} \ \forall s,h \\ &\text{Else } E_{\mathrm{im},s,h} = E_{\mathrm{demand},s,h} + E_{\mathrm{ec},s,h} - E_{\mathrm{fc},s,h} \ \forall s,h \end{aligned} \tag{6}$$

where CAP_{fc} is the installed capacity of the SOFC.

3.4. Following electrical load mode

In the following electrical load (FEL) mode, the system's power output is assumed to follow the electrical demand as much as possible. Since the installed capacity is fixed, shortfalls in generation capacity is met by purchased electricity from grid [36]. Meanwhile, the electric efficiency cannot keep at constant, which is assumed to vary with the part-load ratio. In this mode, the system is operated independently of the end-user's heating or cooling demand. Therefore,

$$\begin{aligned} &\text{If } CAP_{\mathrm{fc}} \geq E_{\mathrm{demand},s,h} \Rightarrow E_{\mathrm{fc},s,h} = E_{\mathrm{demand},s,h} \ \forall s,h \\ &E_{\mathrm{demand},s,h} + E_{\mathrm{ec},s,h} = E_{\mathrm{fc},s,h} + E_{\mathrm{im},s,h} \ \forall s,h \\ &\text{Else } E_{\mathrm{im},s,h} = E_{\mathrm{ec},s,h} + E_{\mathrm{demand},s,h} - E_{\mathrm{fc},s,h} \ \forall s,h \end{aligned} \tag{7}$$

4. Optimal design and dispatch

Unlike the previous fixed sizing option, the installed capacities and dispatch strategy of

231 the proposed system are both unknown. Thus a MINLP model has been established to
232 address the optimal sizing and operation strategy problem simultaneously. The imposed
233 functions and constraints are explained as follows.

234 **4.1. Energy balances**

235 The energy balances consist of electrical balance, heating balance and cooling balance.
236 In the electrical balance, the electrical demand (E_{demand}) is fulfilled by electricity
237 generated from the SOFC (E_{fc}) and/or imported from the grid (E_{im}), less possible
238 consumption by the electrical chiller (E_{ec}) or export to the grid (E_{ex}).

$$\begin{aligned} E_{\text{demand},s,h} &= (1-\delta_{s,h}) \times E_{\text{im},s,h} + E_{\text{fc},s,h} - \delta_{s,h} \times E_{\text{ex},s,h} - E_{\text{ec},s,h} \quad \forall s,h \\ E_{\text{fc},s,h} &= \beta_{\text{fc},s,h} \times PL_{\text{fc},s,h} \times CAP_{\text{fc}} \quad \forall s,h \end{aligned} \tag{8}$$

239 where δ is a binary variable to control the CCHP system interaction with electrical grid,
240 the electricity can be either imported or exported to grid. Other electricity related
241 variables can be calculated by similar constraints as derived in Eq. 3. Compared to the
242 user specified sizing options, the difference is that the CAP_{fc} in this case is a variable
243 while not a fixed value. Since both CAP_{fc} and PL_{fc} are variables and β_{fc} is either 0 or 1,
244 thus the problem requires a non-linear model with mixed integers.

245 The heat demand is fulfilled by the recovered heat from the SOFC, boiler,
246 interaction with heating storage, less possible heat consumption by the absorption
247 chiller, as presented in Eq. 9. The installed capacities of boiler (CAP_{b}) and absorption
248 chiller (CAP_{ac}) are also variables similar with CAP_{fc}.

$$
\begin{aligned}
&Q^{\text{heat}}_{\text{demand},s,h} \le Q^{\text{heat}}_{\text{re},s,h} + Q^{\text{heat}}_{\text{b},s,h} - Q^{\text{heat}}_{\text{st-in},s,h} + Q^{\text{heat}}_{\text{st-out},s,h} - Q^{\text{heat}}_{\text{ac},s,h} \quad \forall s,h \\
&Q^{\text{heat}}_{\text{re},s,h} = \omega \times E_{\text{fc},s,h} \quad \forall s,h \\
&Q^{\text{cool}}_{\text{ac},s,h} = \beta_{\text{ac},s,h} \times CAP_{\text{ac}} \times PL_{\text{ac},s,h} \quad \forall s,h \\
&Q^{\text{cool}}_{\text{b},s,h} = \beta_{\text{b},s,h} \times CAP_{\text{b}} \times PL_{\text{b},s,h} \quad \forall s,h
\end{aligned} \tag{9}
$$

The cooling demand is supplied by either the electrical chiller ($Q^{\text{cool}}_{\text{ec}}$), absorption chiller ($Q^{\text{cool}}_{\text{ac}}$) or both as illustrated in Eq. 10.

$$
\begin{aligned}
&Q^{\text{cool}}_{\text{demand},s,h} \le Q^{\text{cool}}_{\text{ac},s,h} + Q^{\text{cool}}_{\text{ec},s,h} \quad \forall s,h \\
&Q^{\text{cool}}_{\text{ec},s,h} = \beta_{\text{ec},s,h} \times \eta_{\text{ec}} \times E_{\text{ec},s,h} \quad \forall s,h \\
&Q^{\text{cool}}_{\text{ac},s,h} = \beta_{\text{ac},s,h} \times \eta_{\text{ac},s,h} \times Q^{\text{heat}}_{\text{ac},s,h} \quad \forall s,h
\end{aligned} \tag{10}
$$

4.2. Capacity constraint

Each installed device has a capacity limit (CAP^{limit}) which is set as a parameter to cover the peak demand and also prevent over sizing of the installed capacity, and also benefit the model solving time.

$$
\begin{aligned}
&CAP_{\text{fc}} \le CAP^{\text{limit}}_{\text{fc}} \quad \forall s,h \\
&CAP_{\text{b}} \le CAP^{\text{limit}}_{\text{b}} \quad \forall s,h \\
&CAP_{\text{st}} \le CAP^{\text{limit}}_{\text{st}} \quad \forall s,h \\
&CAP_{\text{ec}} \le CAP^{\text{limit}}_{\text{ec}} \quad \forall s,h \\
&CAP_{\text{ac}} \le CAP^{\text{limit}}_{\text{ac}} \quad \forall s,h
\end{aligned} \tag{11}
$$

4.3. Energy storage constraint

Considering that thermal energy is relatively easy and cheap to store, while electricity storage is more expensive, only heat storage is considered in this study. The heat stored in a tank at time *h*+1 is equal to the amount of stored heat at *h* plus the heat charged minus the heat discharged [37]. Heat energy will be lost during the charge/discharge process as well in the tank, thus the efficiencies of η_{st}, $\eta_{\text{st-in}}$ and $\eta_{\text{st-out}}$ are applied, and the heat charge and discharge cannot happen simultaneously by introducing binary variable of α. The storage constraint is presented in Eq. 12.

$$
\begin{aligned}
&Q^{\text{heat}}_{\text{st},s,h1} = Q^{\text{heat}}_{\text{st-init},s} \le CAP^{\text{limit}}_{\text{st}} \ \forall s \\
&Q^{\text{heat}}_{\text{st},s,h} \le CAP^{\text{limit}}_{\text{st}} \ \forall s \text{ and } h \in (2,24) \\
&Q^{\text{heat}}_{\text{st},s,h+1} = \eta_{\text{st}} \times Q^{\text{heat}}_{\text{st},s,h} + \eta_{\text{st-in}} \times Q^{\text{heat}}_{\text{st-in},s,h+1} - \frac{Q^{\text{heat}}_{\text{st-out},s,h+1}}{\eta_{\text{st-out}}} \ \forall s \text{ and } h \in (1,23) \\
&Q^{\text{heat}}_{\text{st},s,h1} = \eta_{\text{st}} \times Q^{\text{heat}}_{\text{st},s,h24} + \eta_{\text{st-in}} \times Q^{\text{heat}}_{\text{st-in},s,h24} - \frac{Q^{\text{heat}}_{\text{st-out},s,h24}}{\eta_{\text{st-out}}} \ \forall s \\
&0 \le Q^{\text{heat}}_{\text{st-in},s,h} \le \alpha_{\text{chr},s,h} \times Q^{\text{limit}}_{\text{st-in}} \ \forall s,h \\
&0 \le Q^{\text{heat}}_{\text{st-out},s,h} \le \alpha_{\text{dis},s,h} \times Q^{\text{limit}}_{\text{st-out}} \ \forall s,h \\
&\alpha_{\text{chr},s,h} + \alpha_{\text{dis},s,h} \le 1 \ \forall s,h
\end{aligned}
\tag{12}
$$

where the heat discharge or charge rates cannot exceed the limit, meanwhile the stored heat in tank must return to the initial state at the end of each day to avoid accumulation. The initial state is a degree of freedom, hence ensuring a cyclic steady state [38].

4.4. On/off constraint

As shown in the previous energy balances, on/off binary variable β and part-load ratio variable *PL* should meet the constraints as shown in Eq. 13, where if the device is on ($\beta = 1$),the minimum output of such device should higher than 30% of its installed capacity to avoid the very low load operation and not higher than 100% of its installed capacity physically [37]. By these groups of constraints, the devices have been modelled to operate closer to practical situations.

$$
\begin{aligned}
&PL_{t,s,h} \ge 0.3 \times \beta_{t,s,h} \ \forall t,s,h \\
&PL_{t,s,h} \le 1 \times \beta_{t,s,h} \ \forall t,s,h
\end{aligned}
\tag{13}
$$

4.5. Start limit constraint

In addition to the on/off constraint, a start limit constraint is also applied by introducing a binary variable φ to avoid switching on and off the device frequently [37]. Since the warm-up of SOFC takes a long time, this constraint is designed to allow only one

277 on-off cycle of the device each day. The constraint can be formulated as:

$$\begin{aligned}
&\sum_{h}\varphi_{\mathrm{fc},s,h} \le 1 \ \forall h,s \\
&\varphi_{\mathrm{fc},s,h+1} \ge \beta_{\mathrm{fc},s,h+1} - \beta_{\mathrm{fc},s,h} \ \forall h,s \\
&\varphi_{\mathrm{fc},s,h+1} \le 1 - \beta_{\mathrm{fc},s,h} \ \forall h,s \\
&\varphi_{\mathrm{fc},s,h+1} \le \beta_{\mathrm{fc},s,h+1} \ \forall h,s
\end{aligned} \tag{14}$$

278 **4.6. Objectives**

279 In this study, two objectives of minimizing annual total cost (ATC) and annual carbon
280 emissions (ACE) have been considered, and the coupled relationships are analyzed
281 using bi-objective optimization. The definition of these two objectives is presented as
282 follows.

283 **4.6.1. Economic objective**

284 The annual total cost (ATC) consists of the cost of purchasing electricity from grid; the
285 revenue of exporting electricity to grid; the operation and maintenance cost of the SOFC,
286 boiler, electrical chiller, absorption chiller, and thermal storage, and the capital cost of
287 each piece of installed equipment [39]. Thus, the ATC can be calculated using Eq. 15:

$$\begin{aligned}
ATC = {} & CRF \times \sum_{t} CAP_{t} \times C^{\mathrm{CAP}} && \text{annualized capital cost} \\
& + \sum_{s,h}\left(\frac{E_{\mathrm{fc},s,h}}{\eta_{\mathrm{fc}}} + \frac{Q^{\mathrm{heat}}_{\mathrm{b},s,h}}{\eta_{\mathrm{b}}}\right) \times C_{NG} && \text{fuel cost} \\
& + \sum_{s,h}\left(E_{\mathrm{fc},s,h} + Q^{\mathrm{heat}}_{\mathrm{b/st},s,h} + Q^{\mathrm{cool}}_{\mathrm{ec/ac},s,h}\right) \times C^{\mathrm{maint}}_{t} && \text{maintenance cost} \\
& - C_{\mathrm{ex}} \times \sum_{s,h} E_{\mathrm{ex},s,h} && \text{revenue of sell electricity} \\
& + C_{\mathrm{im}} \times \sum_{s,h} E_{\mathrm{im},s,h} && \text{grid electricity cost}
\end{aligned} \tag{15}$$

$$CRF = \frac{r \times (1+\mathrm{r})^{n}}{(1+\mathrm{r})^{n} - 1} \tag{16}$$

288 where *CRF* is the capital recovery factor, *r* is the interest rate, and *n* is the project life

289 (years) [40], whose values are provided in Table 1, and other input parameters appeared
290 in Eq. 15 are referring to Table 3.

291 **4.6.2. Emission objective**

292 The annual carbon emission (ACE) is quantified by the emissions from fuel consumed
293 plus the electricity purchased from grid as defined in Eq. 17.

$$\begin{aligned} ACE = {} & \partial_{\mathrm{NG}} \times \sum_{s,h} \left(\frac{E_{\mathrm{fc},s,h}}{\eta_{\mathrm{fc}}} + \frac{Q_{\mathrm{b},s,h}^{\mathrm{heat}}}{\eta_{\mathrm{b}}} \right) && \text{natural gas emission} \\ & + \partial_{\mathrm{grid}} \times \sum_{s,h} E_{\mathrm{im},s,h} && \text{purchasing electricity emission} \end{aligned} \tag{17}$$

294 where ∂_{NG} and ∂_{grid} are the emission factors of natural gas and the grid respectively,
295 which quantifies the global warming impact of a mixture of emissions mainly including,
296 but not limited to, CO_2, CH_4, and NO_x, whose values are referring to Table 1.

297

298 **5. Multi-objective optimization**

299 Generally, multi-objective optimization represents more than one objective. Since two
300 objectives (ATC and ACE) have been considered in this study, the problem is bi-
301 objective. Several approaches can be applied to solve the multi-objective optimization
302 problem such as: Weighted Sum, Goal Programming and $\mathcal{E}$-constraint method [41, 42].
303 In this study, the $\mathcal{E}$-constraint method is applied to identify the non-dominated optimal
304 solution set for such problem, and previous study has demonstrated that the optimal
305 points identified by $\mathcal{E}$-constraint method are global optimal points correspondingly [43].
306 The non-dominated concept is introduced firstly before the description of $\mathcal{E}$-constraint
307 method. Taking bi-objective minimization problem as an example as illustrated in Fig.

3, it is observed that no more point exists at the bottom-left side of the Pareto frontier, indicating there is no better solution where the values of two objectives are both less than that of the points on the Pareto frontier simultaneously [44]. Hence, by utilization of $\mathcal{E}$-constraint method, the most desired (Ideal) point and the least desired (Nadir) point can be determined for each objective through single objective optimizations. Then one of the objectives can be discretized into several segments and converted to constraints, and another objective has to be optimized within the inequality constraints of the previous objective. All feasible solutions identified by such method can be displayed as a Pareto frontier as sketched in Fig. 3.

In this study, the proposed MINLP model is developed in GAMS 24.0 [45] on a PC with an Intel (R) Core (TM) i5-4590 CPU, 3.30 GHz CUP and 8.0 GB of RAM, and the results are solved by the LINDO solver. LINDO is one of the advanced commercial solvers, whose core is Generalized Reduced Gradient (GRG) algorithm [46]. To ensure the global optimum when the model is non-linear and non-convex, the Global options is applied with multi-start capability. Instead of stopping at one local optimal location, the Global solver will search until the global optimum is confirmed within certain time limit. Then by implementing $\mathcal{E}$-constraint method, the entire Pareto solution set can be obtained, and an explanative flow chart of model solving procedure is presented in Fig. 4.

Once the Pareto frontier is found, two well-known decision making approaches of LINMAP (Linear Programming Technique for Multidimensional Analysis of

329 Preference) and TOPSIS (Technique for Order of Preference by Similarity to Ideal
330 Solution) are applied to identify and verify the bi-optimal solution as described in the
331 following section [47].

332 **5.1. Decision making**

333 In multi-objective optimization problems, the optimal solution selection procedure is
334 more complicated than in single-objective optimization problems. Each Pareto-optimal
335 solution represents a compromise considering different objectives, thus the component
336 of the corresponding vector of objectives cannot simultaneously be improved [48].
337 Thus the decision making approaches for identifying the most desired route from all
338 accessible routes obtained from the multi-objective optimization play a vital role.
339 Meanwhile, as the scales and dimensions of the objectives are different (one objective
340 is cost, another is carbon emission), only the non-dimensioned decision making
341 techniques can be applied. In this study, two most recognized decision making
342 approaches of LINMAP and TOPSIS were applied and described as follows.

343 **5.1.1 LINMAP approach**

344 In the LINMAP decision approach, the search space is introduced firstly through single-
345 objective optimizations of two different objectives respectively. Then the “Ideal” point
346 is introduced and the location of ideal point is defined at the optimal latitude and
347 longitude existed in the search space. Since the trade-off exists between two objectives
348 and all points on the Pareto frontiers are non-dominated, the “Ideal” point cannot be
349 located on the Pareto frontier as illustrated in Fig. 3. By LINMAP approach, the

Euclidian distance (ED_{i+}) between each point in the Pareto frontier, and the ideal point, is determined as defined in Eq. 18, and the point in the Pareto frontier with the shortest Euclidian distance is the prior optimal point. More details about the LINMAP approach is provided in [49].

$$ED_{i+} = \sqrt{\sum_{j=1}^{n} (f_{ij}^{\text{norm}} - f_{j}^{\text{ideal}})^2} \tag{18}$$

where i denotes the index of each solution on the Pareto frontier, and j is the index of the considered objective.

5.1.2 TOPSIS approach

In the TOPSIS approach, the "Nadir" point is also introduced which is located at the worst place of the search space. Thus, the Euclidian distance (ED_{i-}) between each point on the Pareto frontier and the nadir point can be determined as shown in Eq. 19. Then, a new assessment (Y_i) is defined as Eq. 20, thus the solution with maximum Y_i is considered as the most desired solution [47-49].

$$ED_{i-} = \sqrt{\sum_{j=1}^{n} (f_{ij}^{\text{norm}} - f_{j}^{\text{nadir}})^2} \tag{19}$$

$$Y_i = \frac{ED_{i-}}{ED_{i-} + ED_{i+}} \tag{20}$$

Note that for both Euclidean non-dimensioned approaches of LINMAP and TOPSIS, the solutions at the Pareto frontier should be normalized by Eq. 21 and 22 before calculating the Euclidian distance.

$$f_{ij}^{\text{norm}} = \frac{f_{ij} - \min(f_{ij})}{\max(f_{ij}) - \min(f_{ij})} \quad \text{for maximization objectives} \tag{21}$$

$$f_{ij}^{\text{norm}} = \frac{\max(f_{ij}) - f_{ij}}{\max(f_{ij}) - \min(f_{ij})} \quad \text{for minimization objectives} \tag{22}$$

6. Case study

In this section, the proposed model for optimal design and dispatch of SOFC based CCHP system is applied to a case study of a hospital located in Shanghai, which is in the 'hot summer, cold winter' climate zone of China. The coldest month is January and the hottest month is July. The hospital has a total ground floor area of 35,100 m^2, and the energy demand of the hospital is relatively stable due to the 24 hours' operation schedule. As shown in Fig. 5 (a) (b) and (c), spring and fall are considered as the transition season, thus a year can be divided into three periods: summer, winter and transition. Although the prediction of the demand profiles is a challenging problem, the focus of this study is the optimization model. Thus the hourly energy demand profiles of typical days during three periods are obtained from the energy audit of corresponding building, which are considered as the representative energy demand profiles over corresponding periods. In addition, the time-of-use energy prices have been presented in Fig. 5 (d).

6.1. Technical, economic and environmental input parameters

The input parameters of the optimization model have significant impacts on the optimal results, thus the state-of-the-art technical, economic and environmental input parameters are carefully given in this section. Table 1 lists the general project assumptions as well as the carbon emission factors particular for the case study in China, thus the carbon emissions from purchased electricity and fuel consumptions can be

386 quantified as derived by Eq. 17. The technical input parameters including the
387 efficiencies and maximum capacities with assumptions are presented in Table 2.

388 In addition, the capital cost and maintenance cost of major devices are listed in
389 Table 3, where capital cost is related to the installed capacity, and maintenance cost is
390 proportional to the energy produced. It is noteworthy that the prediction of the SOFC
391 capital cost is difficult [23, 51]. The cost ranges from the unsubsidized of $12,000/kW
392 to $2,500/kW considering the cost projections for value of $1/5^{th}$ when the technology
393 appears in the market and the production reaches a greater scale [23, 51], Therefore, the
394 capital cost of $3,000/kW is assumed in this study considering the subsidies from
395 government for clean energy promotion similar with solar PV and wind power
396 technologies. In addition, a fixed value of $1,200/kW is assumed for the stack
397 replacement at the 5^{th} year of the project [23], and the maintenance cost of the SOFC is
398 assumed to be $0.02/kW [52].

399

400 **7. Results and discussion**

401 In this study, each optimization takes an average runtime of 1,100 seconds, then all
402 optimization results are sorted and plotted as different Pareto frontiers based on the
403 design and dispatch options as mentioned, then LINMAP and TOPSIS decision-making
404 approaches are applied to identify the bi-objective most desired solution. In this section,
405 the calculation results are analyzed from different perspectives to illustrate the
406 effectiveness of the proposed model and approaches: 1) plot the Pareto frontiers and

407 determine the multi-objective optimal solutions, 2) compare the system design and
408 operation parameters under different scenarios, 3) exhibit the energy balances to show
409 the impacts of different optimization objectives, 4) analyze the operation and capital
410 cost difference of each scenario, 5) demonstrate the competitiveness of proposed
411 SOFC-CCHP system through the levelized cost of energy, 6) evaluate the
412 environmental benefits.

413 **7.1. Pareto frontiers and decision approaches**

414 **7.1.1. Pareto frontiers**

415 Firstly, both the fixed sizing options and the optimal sizing options are applied for the
416 case study and Fig. 6 presents the Pareto frontiers of all optimal solutions for each
417 option to achieve the least annual total cost (ATC), least annual carbon emissions (ACE)
418 or both. For each Pareto frontier, both LINMAP and TOPSIS decision making
419 approaches were utilized to identify the most desired solution from every optimal
420 solution and three points for each Pareto frontier have been marked with letters,

421 - Letters A, B, C, D, E represent optimal sizing, fixed sizing with full-load, day/night,
422 baseload, and following electrical load modes respectively,

423 - Number 1, 2, 3 indicate the optimization to achieve the least ATC objective, the
424 least ACE objective, and the bi-objective.

425 A significant difference of ATC and ACE can be observed for the optimal sizing
426 option and the fixed sizing options with different operation strategies as shown in Fig.
427 6. In the optimal sizing option (shown in blue), the installed capacities of each device

are optimized, which leads to significant saving of capital cost, thus lower ATC can be achieved compared to the fixed sizing options. Meanwhile, by optimal dispatch of the system with the least emission objective, a lower ACE can be achieved compared to fixed sizing options, but the ACE gap between optimal sizing option (A2) and the fixed sizing with FEL mode (E2) is not very large. Considering four fixed sizing options only, the following electrical load (in purple) mode can achieve the least ACE compared to other dispatch strategies due to the effective use of SOFC. When fuel cell is operated in full load (FL) mode (in green), the SOFC output keeps at full capacity, thus the surplus electricity is generated and sold back to grid, which leads to the least ATC compared to other fixed sizing options. But the emission of FL mode is larger than FEL mode since the emission of surplus electricity is also taken into account. In addition, since the SOFC output keeps at full load, significant amount of heat along with the power generation can be recovered. Thus the cooling and heating demand can be fulfilled by such recovered heat to a large extent, which further results in a relatively tiny search space of two objectives. Therefore, a zoom-in view of FL mode Pareto frontier is also presented. Besides, the system operated at Day/night (D/N) shifting mode achieves moderate performance for both cost and emission objectives as plotted in red, and baseload (in yellow) mode turns out to be least desired dispatch strategy which does not make full use of the fuel cell advantages but bears the high installation cost.

7.1.2. LINMAP and TOPSIS results

As mentioned above, Number 1 and 2 represent single objective optimization results, meanwhile Number 3 indicates the bi-objective optimized solution for which the location on the Pareto frontier is determined by LINMAP and TOPSIS approaches. The details of the two decision making approaches have been presented by the values of normalized ED_{i+} and Y_i as shown in Fig. 7. The normalized values of ED_{i+} and Y_i for each option have been marked by certain colors in consistent with Fig. 6. It can be seen that two approaches draw similar conclusions in most cases (the smaller ED_{i+}, the better; the larger Y_i, the better). The only exception happens at full load (FL) operation, where both the normalized ED_{i+} and Y_i value differences are not significant (in green), the reason is that the search space is small enough (within 1%) as explained in last paragraph and shown in Fig. 6 (in green as well), thus each solution on the Pareto frontier could be considered as the representative of the most desired solution.

7.2. Baseline and comparison

With the optimization results obtained by both single objective optimization and bi-objective optimization in the last section, the technical and energy performance was evaluated, as well as compared to the baseline condition of the traditional energy system as listed in Table 4. In the baseline condition, it is assumed that the electrical demand is fulfilled by imported electricity from the grid, heating and cooling demand is supplied by boiler and electrical chiller respectively, thus the installed capacity of boiler and electrical chiller must be higher than the maximum energy demand of the year.

Overall 13 desired solutions have been listed in Table 5, which is consistent as

illustrated in Fig. 6. It is noticed that only one point (Point B) has been selected to represent the most desired solution of full load dispatch strategy as explained in last two sections. It can be seen from Table 5 that:

1) The installed capacity of each device has been optimized which is generally less than the fixed sizing options, which reduces the capital cost remarkably and further leads to the reduction of annual total cost.

2) Considering the optimal sizing options, in order to achieve lower carbon emissions, larger capacities of fuel cell and absorption chiller would be installed reflecting the environmental advantage of these technologies. By contrast, to achieve the least annual total cost, the installed capacity of the SOFC and absorption chiller are smaller. Meanwhile, larger capacity of electrical chiller is installed due to the relatively cheap capital cost and the higher COP (coefficient of performance).

3) Considering the four fixed sizing options, the biggest amount of excess electricity would be generated and exported to grid when the system is operated in full load mode. By contrast, a system operating at baseload mode would not generate excess electricity and hence would rely on grid electricity import to a large extent compared to other modes. Day/night operation mode has the most frequent interactions with the grid. The following electrical load mode set the system power output equal to electrical load, thus no extra electricity would be produced and electricity imported from grid may be needed when the cooling load is big enough.

7.3. Energy balances

To better exhibit the results of optimal design and dispatch by the proposed model, the hourly basis electrical, heating, and cooling balances of selected solutions have been presented in this section. Due to the space limitation, Fig. 8 presents the summer electrical balances of representative cases including the optimal sizing option with the objective to achieve the least ATC (A1), optimal sizing option for minimum ACE (A2), fixed sizing with full load dispatch strategy (B) and fixed sizing with following electrical load mode (E1). It can be seen that, in order to achieve the least ATC as shown in (a), the installed capacity of fuel cell is less than other options due to the high capital cost of the SOFC, thus more electricity has to be imported from grid so as to fulfill the electrical demand as well as the cooling demand. Comparing (b) with (a), a larger capacity fuel cell would be installed since the fuel cell has better environmental performance than the grid. As for (c), the output of fuel cell stays at full capacity thus only small amounts of electricity would be imported to power the electrical chiller to fulfill the cooling demand in the cooling peak period, and during the rest of the period, electricity would be exported to grid to reduce cost. In addition, the fuel cell power output follows the electrical load as shown in (d), thus no electricity would be exported to grid.

Fig. 9 shows the summer cooling balances of selected options. For the A1 option, less capacity of absorption chiller (AC cooling) would be installed to save capital cost compared to A2 option, where recovered energy would be fully utilized thus significant amount of cooling comes from the absorption chiller and the insufficient cooling

demand is supplied by electrical chiller as shown in (b). In addition, the absorption chiller would be applied during the electricity peak price period to save operating cost for both (c) and (d) options, while during the electricity off-peak price period, the dispatch strategy is determined by comprehensively considering the impacts of electrical cost, maintenance cost, efficiency of electrical and absorption chillers, and the on/off constraints.

Fig. 10 illustrates the winter heating balances of same options. By comparison of A1 (a) and A2 (b), the thermal storage would be utilized more frequently by A2, which can be explained by the larger installed capacity of the fuel cell in A2 and the corresponding larger heat output of fuel cell, meanwhile extra heat would be stored for later usage so as to achieve higher carbon reduction. In addition, when the system is operated at full load mode, the heat output from the fuel cell is fixed, thus when the heating load is low (2 to 7 a.m.), the extra heat would be stored and released when heating demand grows (8 a.m.). As for the following electrical load operation mode (d), the heat supply from fuel cell is dependent on the electrical output and is lower than the heating demand, thus the insufficient heating demand would be fulfilled by the boiler.

7.4. Cost breakdown

To better understand the project economics from the life cycle perspective, as well as compared to the baseline situation, the ten years' project operation cost (OPEX) of the proposed system as well as the capital cost are discussed in this section.

7.4.1 OPEX

The selected solutions of different sizing and dispatch strategies with the objective to achieve the least annual total cost have been illustrated in Fig. 11. Compared to the baseline system, the energy consumption pattern changed significantly in that the majority of cost shifts from purchasing electricity to natural gas. Meanwhile, the radar surface area represents the amount of the operation cost (OPEX). By implementing SOFC based CCHP system, the OPEX can be reduced by 27%, 28%, 27%, 14%, and 24% for A1, B, C1, D1, E1 points respectively. The main reason is that the SOFC has outstanding electrical efficiency, furthermore, the waste heat along with the power generation is recovered and cascade utilized by the proposed CCHP system, thus OPEX can be saved.

7.4.2. Capital cost

As shown in Fig. 12, significant savings of capital cost can be achieved by optimal sizing compared to fixed sizing options. The solution with minimized ATC (as shown in A1) would save 61% of capital investment compared to fixed sizing options from B to E3. Among all options, fuel cell capital cost accounts for over 78% of the total investment, thus the fuel cell capital cost would have vital impact on the project economics.

7.5. Levelized cost of energy

In this study, the levelized cost of energy (LCOE) is introduced to quantify the project economics from an entire project lifespan perspective [54], which is defined as the total project cost per unit of produced electricity, heat or cooling as shown in Eq. 23. This

figure is often quantified in units of $/kWh for comparison with utility industry standards. Note that heat and cooling energy has different energy grades compared to electricity, which would be converted to equivalent electricity by conversion factors (0.23 for heat supply water and 0.07 for chilled water) [55].

$$LCOE = \frac{C_{\text{total}}}{E + Q^{\text{cool}} + Q^{\text{heat}}} = \frac{C_{\text{total}}}{E + \mu_{\text{cool}} \times Q^{\text{cool}} + \mu_{\text{heat}} \times Q^{\text{heat}}} \quad (23)$$

Thus, the project lifespan cost breakdown and LCOE can be concluded as shown in Fig. 13. Compared to the baseline energy system performance with LCOE of 0.21 $/kWh, the proposed SOFC based CCHP system design and dispatch at A1~A3, B, C1~C3 options can achieve acceptable LCOE. Particularly, the entire project cost can be significantly reduced and the most investment attractive option is optimal sizing and dispatch with the objective to achieve minimum ATC with the LCOE of 0.17 $/kWh (as shown in point A1). Therefore, from the LCOE perspective, the proposed SOFC based CCHP system is financially feasible based on the state-of-the-art input parameters. Moreover, with the continuous development of fuel cell technology, the capital cost would be further reduced, which may make the technology more attractive to investors in the near future.

7.6. Environmental benefit

In addition to economic analysis, the environmental benefit of SOFC based CCHP systems has also been evaluated. As shown in Fig. 14, significant amounts of carbon emission can be saved with the reduction ranging from 54% (A1 solution) to 61% (A2 solution). Among all options, the least annual carbon emissions (ACE) is achieved by

optimal sizing with the objective of reducing carbon emission (A2 solution) as expected, meanwhile in order to achieve the least operating cost (A1 solution), relatively large amount of electricity would be imported from grid due to the cheap electrical price during the off-peak period, thus the carbon emissions would be relatively high compared to the A2 solution. When the system is operated at full load, the majority of the carbon emissions come from the fuel cell natural gas and require the least amount of electricity from grid. If the system is operated at baseload mode, significant amounts of electricity are still needed as expected. In general, the electrical load following mode is the most carbon emission saving among the four types of dispatch strategies, and carbon emission can be further reduced by optimal sizing, but the amount is not significant.

8. Conclusions

In this study, an MINLP (Mixed Integer Non-linear Programming) model has been established for optimal design and dispatch SOFC (solid oxide fuel cell) based CCHP (combined cooling heating and power) systems. Two sizing options of user specified and optimal sizing are achieved and compared. The proposed model also enables four types of operation strategies, and further introduces equipment on/off, and number of start constraints to make the model more realistic. The economic and environmental single objective optimizations have been addressed. Furthermore, the multi-optimization has been achieved by the $\mathcal{E}$-constraint approach. The optimization results

595 of each option are presented as Pareto frontiers and the most desired solution has been
596 identified and verified by the two decision making approaches of LINMAP and
597 TOPSIS. The model has been implemented on the case study of a hospital in Shanghai,
598 China considering the state-of-the-art technical parameters, time-of-use energy prices
599 and carbon emission factors. The optimal results with trade-off between cost and
600 emission are obtained and several key conclusions can be drawn as follows:

601 1) The proposed model enables two sizing options which make it more flexible for
602 users. Using the optimal sizing option, the installed capacity of each device would
603 be optimized with a 61% saving of capital cost compared to the fixed sizing option,
604 which makes the project more attractive financially.

605 2) The $\mathcal{E}$-constraint method turns out to be an effective method to deal with more than
606 one conflicting objectives. By integration of the proposed MINLP model with the
607 $\mathcal{E}$-constraint method, the optimal Pareto frontier can be plotted, which can provide
608 valuable guidance of the tradeoff between economic and environmental
609 perspectives for decision makers. In addition, the compromised solutions for
610 studied options have been identified and verified by two decision making
611 approaches of LINMAP and TOPSIS. The results indicate that both decision
612 making methods have similar outcomes in most of the cases, while exceptions may
613 be observed when the search space is too narrow.

614 3) The analysis of project cost breakdown illustrates that the fuel cell high capital cost
615 accounting for 19%~30% of the project total cost. However, the levelized cost of

energy (LCOE) calculation indicates that the LCOE as low as 0.17 $/kWh can be achieved by the optimal design and dispatch of SOFC based CCHP systems through the proposed modelling, which is lower than the baseline system with a LCOE of 0.21 $/kWh.

4) The environmental benefit of implementing SOFC based CCHP is significant as well, with the optimal 61% of carbon emission reduction. Thus to slow down the global warming, the policy makers should pay more attention to developing and promoting this kind of green technology.

Overall, the proposed methodology is generic and provides the framework to optimize the design and dispatch of SOFC based CCHP system with bi-objectives. Future work may consider integration with renewable energy sources to further reduce the environmental impact and achieve greater cost reduction.

Acknowledgement

The research has received the support from National Natural Science Foundation of China under grant No. 51206137. The authors are also grateful to the Fundamental Research Fund for the Central Universities with grant No. 20720150111.

Reference

[1] Kamilaris A, Kalluri B, Kondepudi S, Kwok Wai T. A literature survey on measuring energy usage for miscellaneous electric loads in offices and commercial buildings. Renewable and Sustainable Energy Reviews. 2014;34:536-50.

[2] Zhang J, Cho H, Knizley A. Evaluation of financial incentives for combined heat and power (CHP) systems in U.S. regions. Renewable and Sustainable Energy Reviews. 2016;59:738-62.

[3] Li M, Mu H, Li N, Ma B. Optimal design and operation strategy for integrated evaluation of CCHP (combined cooling heating and power) system. Energy. 2016;99:202-20.

[4] Fubara TC, Cecelja F, Yang A. Modelling and selection of micro-CHP systems for domestic energy supply: The dimension of network-wide primary energy consumption. Applied Energy. 2014;114:327-34.

[5] Elmer T, Worall M, Wu S, Riffat SB. Fuel cell technology for domestic built environment applications: State of-the-art review. Renewable and Sustainable Energy Reviews. 2015;42:913-31.

[6] Ellamla HR, Staffell I, Bujlo P, Pollet BG, Pasupathi S. Current status of fuel cell based combined heat and power systems for residential sector. Journal of Power Sources. 2015;293:312-28.

[7] Pade L-L, Schröder ST. Fuel cell based micro-combined heat and power under different policy frameworks – An economic analysis. Energy Conversion and Management. 2013;66:295-303.

[8] Ghadimi P, Kara S, Kornfeld B. The optimal selection of on-site CHP systems through integrated sizing and operational strategy. Applied Energy. 2014;126:38-46.

[9] Wang J, Mao T, Dou C. Configuration Optimization with Operation Strategy of Solar-assisted Building Cooling Heating and Power System to Minimize Energy Consumption. Energy Procedia. 2016;88:742-7.

[10] Kang L, Yang J, An Q, Deng S, Zhao J, Wang H, et al. Effects of load following operational strategy on CCHP system with an auxiliary ground source heat pump considering carbon tax and electricity feed in tariff. Applied Energy. 2017;194:454-66.

[11] Najafi B, Haghighat Mamaghani A, Rinaldi F, Casalegno A. Long-term performance analysis of an HT-PEM fuel cell based micro-CHP system: Operational strategies. Applied Energy. 2015;147:582-92.

[12] Sorace M, Gandiglio M, Santarelli M. Modeling and techno-economic analysis of the integration of a FC-based micro-CHP system for residential application with a heat pump. Energy. 2017;120:262-75.

[13] Wei D, Chen A, Sun B, Zhang C. Multi-objective optimal operation and energy coupling analysis of combined cooling and heating system. Energy. 2016;98:296-307.

[14] Wu Q, Ren H, Gao W, Ren J. Multi-criteria assessment of building combined heat

673 and power systems located in different climate zones: Japan–China comparison. Energy.
674 2016;103:502-12.
675 [15] Rillo E, Gandiglio M, Lanzini A, Bobba S, Santarelli M, Blengini G. Life Cycle
676 Assessment (LCA) of biogas-fed Solid Oxide Fuel Cell (SOFC) plant. Energy.
677 2017;126:585-602.
678 [16] Ranjbar MR, Mohammadian M, esmaili S. Economic analysis of hybrid system
679 consists of fuel cell and wind based CHP system for supplying grid-parallel residential
680 load. Energy and Buildings. 2014;68:476-87.
681 [17] Chen X, Gong G, Wan Z, Zhang C, Tu Z. Performance study of a dual power
682 source residential CCHP system based on PEMFC and PTSC. Energy Conversion and
683 Management. 2016;119:163-76.
684 [18] Wouters C, Fraga ES, James AM. An energy integrated, multi-microgrid, MILP
685 (mixed-integer linear programming) approach for residential distributed energy system
686 planning – A South Australian case-study. Energy. 2015;85:30-44.
687 [19] Yang Y, Zhang S, Xiao Y. An MILP (mixed integer linear programming) model
688 for optimal design of district-scale distributed energy resource systems. Energy.
689 2015;90:1901-15.
690 [20] Fong KF, Lee CK. Investigation on zero grid-electricity design strategies of solid
691 oxide fuel cell trigeneration system for high-rise building in hot and humid climate.
692 Applied Energy. 2014;114:426-33.
693 [21] Pellegrino S, Lanzini A, Leone P. Techno-economic and policy requirements for
694 the market-entry of the fuel cell micro-CHP system in the residential sector. Applied
695 Energy. 2015;143:370-82.
696 [22] Facci AL, Cigolotti V, Jannelli E, Ubertini S. Technical and economic assessment
697 of a SOFC-based energy system for combined cooling, heating and power. Applied
698 Energy. 2017;192:563-74.
699 [23] McLarty D, Brouwer J, Ainscough C. Economic analysis of fuel cell installations
700 at commercial buildings including regional pricing and complementary technologies.
701 Energy and Buildings. 2016;113:112-22.
702 [24] Adam A, Fraga ES, Brett DJL. Options for residential building services design
703 using fuel cell based micro-CHP and the potential for heat integration. Applied Energy.
704 2015;138:685-94.
705 [25] Hamed AR, Mousa M, Armin E, Omid P. Thermodynamic and economic
706 optimization of SOFC-GT and its cogeneration opportunities using generated syngas
707 from heavy fuel oil gasification. Energy. 2016;107:141-164.
708 [26] Andrea LF, Viviana C, Elio J, Stefano U. Technical and economic assessment of
709 a SOFC-based energy system for combined cooling, heating and power. Applied
710 Energy. 2017;192:563-574.
711 [27] Zhang SQ, Liu HL, Liu ML, Sakaue E, Li N, Zhao YR. An efficient integration
712 strategy for a SOFC-GT-SORC combined system with performance simulation and

parametric optimization. Applied Thermal Engineering. 2017;121:314-324.

[28] Lorenzo GD, Corigliano O, Faro ML, Frontera P, Antonucci P, Zignani SC, Trocino S, Mirandola FA, Arico AS, Fragiacomo P. Thermoelectric characterization of an intermediate temperature solid oxide fuel cell system directly fed by dry biogas. Energy Conversion and Management. 2016;127:90-102.

[29] Shariatzadeh OJ, Refahi AH, Rahmani M, Abolhassani SS. Economic optimisation and thermodynamic modelling of SOFC tri-generation system fed by biogas. Energy Conversion and Management. 2015;105:772-781.

[30] Mehr AS, Mahmoudi SMS, Yari M, Chitsaz A. Thermodynamic and exergoeconomic analysis of biogas fed solid oxide fuel cell power plants emphasizing on anode and cathode recycling: A comparative study. Energy Conversion and Management. 2015;105:596-606.

[31] Hawkes AD, Aguiar P, Croxford B, Leach MA, Adjiman CS, Brandon NP. Solid oxide fuel cell micro combined heat and power system operating strategy: Options for provision of residential space and water heating. Journal of Power Sources. 2007;164:260-71.

[32] Pade L-L, Schröder ST, Münster M, Birkl C, Ropenus S, Morthorst PE, et al. Policy schemes, operational strategies and system integration of residential co-generation fuel cells. International Journal of Hydrogen Energy. 2013;38:3050-63.

[33] US DOE Hydrogen and Fuel Cells Program: DOE Fuel Cell Power Analysis. FC Power Model Solid Oxide Fuel Cell, version 2.0. 2017.
https://www.gams.com/latest/docs/userguides/index.html [Access: 2017/05/01].

[34] Ameri M, Besharati Z. Optimal design and operation of district heating and cooling networks with CCHP systems in a residential complex. Energy and Buildings. 2016;110:135-148.

[35] Chen Y, Zhang TT, Yang HX, Peng JQ. Study on energy and economic benefits of converting a combined heating and power system to a tri-generation system for sewage treatment plants in subtropical area. Applied Thermal Engineering. 2016;94:24-39.

[36] Chen JMP, Ni M. Economic analysis of a solid oxide fuel cell cogeneration/trigeneration system for hotels in Hong Kong. Energy and Buildings. 2014;75:160-9.

[37] Bischi A, Taccari L, Martelli E, Amaldi E, Manzolini G, Silva P, et al. A detailed MILP optimization model for combined cooling, heat and power system operation planning. Energy. 2014;74:12-26.

[38] Zhang D, Shah N, Papageorgiou LG. Efficient energy consumption and operation management in a smart building with microgrid. Energy Conversion and Management. 2013;74:209-22.

[39] Eriksson ELV, Gray EM. Optimization and integration of hybrid renewable energy hydrogen fuel cell energy systems – A critical review. Applied Energy. 2017;202:348-

64.

[40] Bracco S, Dentici G, Siri S. Economic and environmental optimization model for the design and the operation of a combined heat and power distributed generation system in an urban area. Energy. 2013;55:1014-24.

[41] Cui YF, Geng ZQ, Zhu QX, Han YM. Review: Multi-objective optimization methods and application in energy saving. Energy. 2017;125:681-704.

[42] Al-falahi MDA, Jayasinghe SDG, Enshaei H. A review on recent size optimization methodologies for standalone solar and wind hybrid renewable energy system. Energy Conversion and Management. 2017;143:252-274.

[43] De-León Almaraz S, Azzaro-Pantel C, Montastruc L, Boix M. Deployment of a hydrogen supply chain by multi-objective/multi-period optimisation at regional and national scales. Chemical Engineering Research and Design. 2015;104:11-31.

[44] Feng Y, Zhang Y, Li B, Yang J, Shi Y. Comparison between regenerative organic Rankine cycle (RORC) and basic organic Rankine cycle (BORC) based on thermoeconomic multi-objective optimization considering exergy efficiency and levelized energy cost (LEC). Energy Conversion and Management. 2015;96:58-71.

[45] GAMS Development Corporation. GAMS - A User's Guide. 2017. https://www.gams.com/latest/docs/userguides/index.html [Access: 2017/05/01].

[46] LINDO Systems Inc. LINDO API – User Manual. 2017. http://www.lindo.com/index.php/help/user-manuals [Access: 2017/05/01].

[47] Han J-H, Ryu J-H, Lee I-B. Multi-objective optimization design of hydrogen infrastructures simultaneously considering economic cost, safety and CO2 emission. Chemical Engineering Research and Design. 2013;91:1427-39.

[48] Feng Y, Hung T, Zhang Y, Li B, Yang J, Shi Y. Performance comparison of low-grade ORCs (organic Rankine cycles) using R245fa, pentane and their mixtures based on the thermoeconomic multi-objective optimization and decision makings. Energy. 2015;93:2018-29.

[49] Zhang D, Evangelisti S, Lettieri P, Papageorgiou LG. Economic and environmental scheduling of smart homes with microgrid: DER operation and electrical tasks. Energy Conversion and Management. 2016;110:113-24.

[50] Zeng R, Li H, Jiang R, Liu L, Zhang G. A novel multi-objective optimization method for CCHP–GSHP coupling systems. Energy and Buildings. 2016;112:149-58.

[51] Wei M, Smith SJ, Sohn MD. Experience curve development and cost reduction disaggregation for fuel cell markets in Japan and the US. Applied Energy. 2017;191:346-57.

[52] Strazza C, Borghi AD, Costamagna P, Gallo M, Brignole E, Girdinio P. Life Cycle Assessment and Life Cycle Costing of a SOFC system for distributed power generation. Energy Conversion and Management. 2015;100:64-77.

[53] Luo Z, Wu Z, Li ZY, Cai HY, Li BJ, Gu W. A two-stage optimization and control for CCHP microgrid energy management. Applied Thermal Engineering.

2017;125:513-522.

[54] Reichelstein S, Yorston M. The prospects for cost competitive solar PV power. Energy Policy. 2013;55:117-27.

[55] Yang C, Yang Z, Cai R. Comparison of CCHP Efficiencies Based on Off-design Characteristics. Proceedings of the CSEE. 2008;02:8-13. [In Chinese].

Figure captions:

Fig. 1. Superstructure of SOFC-CCHP building energy system.

Fig. 2. Logic flow chart of the study.

Fig. 3. Illustration of non-dominated and bi-objective decision making approaches.

Fig. 4. Flow chart of multi-objective MINLP model solving procedure.

Fig. 5. Energy demand profiles of summer (a) winter (b) transition season (c) and energy prices (d).

Fig. 6. Pareto frontiers for each sizing option and dispatch strategies.

Fig. 7. LINMAP and TOPSIS decision making details.

Fig. 8. Summer electrical balances of A1 (a) A2 (b) B (c) and E1 (d) optimal solutions (A1-optimal sizing with objective of the least ATC, A2-optimal sizing with objective of the least ACE, B-fixed sizing with full load operation mode, E1- fixed sizing with following electrical load operation mode).

Fig. 9. Summer cooling balances of A1 (a) A2 (b) B (c) and E1 (d) optimal solutions.

Fig. 10. Winter heating balances of A1 (a) A2 (b) B (c) and E1 (d) optimal solutions.

Fig. 11. Radar figure of OPEX breakdown comparison.

Fig. 12. Capital cost breakdown comparison.

Fig. 13. Project total cost breakdown and LCOE comparison.

Fig. 14. Annual carbon emission comparison of each options.

Table captions：

Table 1. Project general information and emission factor.

Table 2. Technical input parameters of major components.

Table 3. Economic input parameters of major components.

Table 4. Baseline condition system capacity and performance.

Table 5. System design and performance comparison of each point.

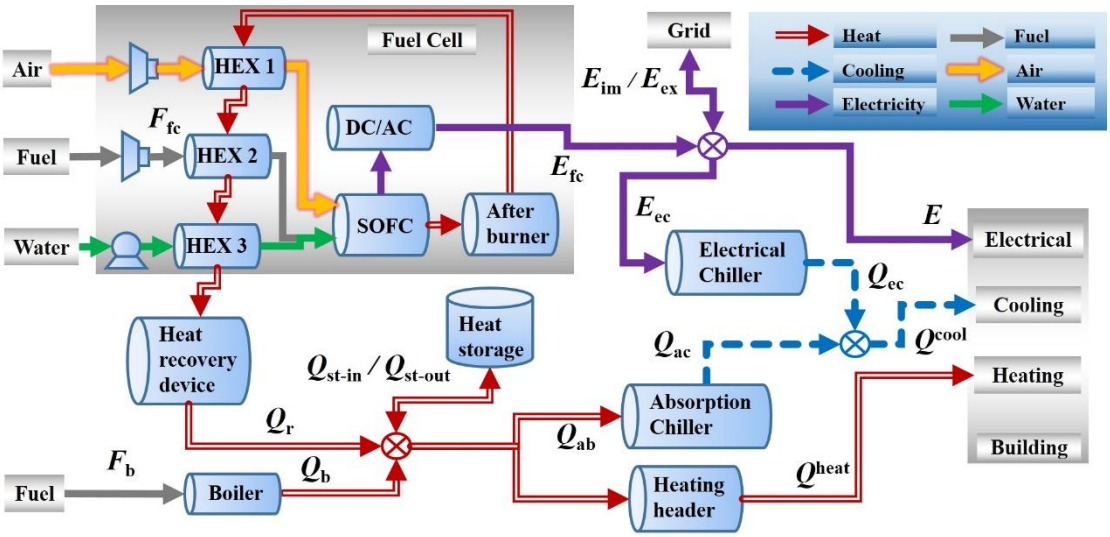

Fig. 1. Superstructure of SOFC-CCHP building energy system.

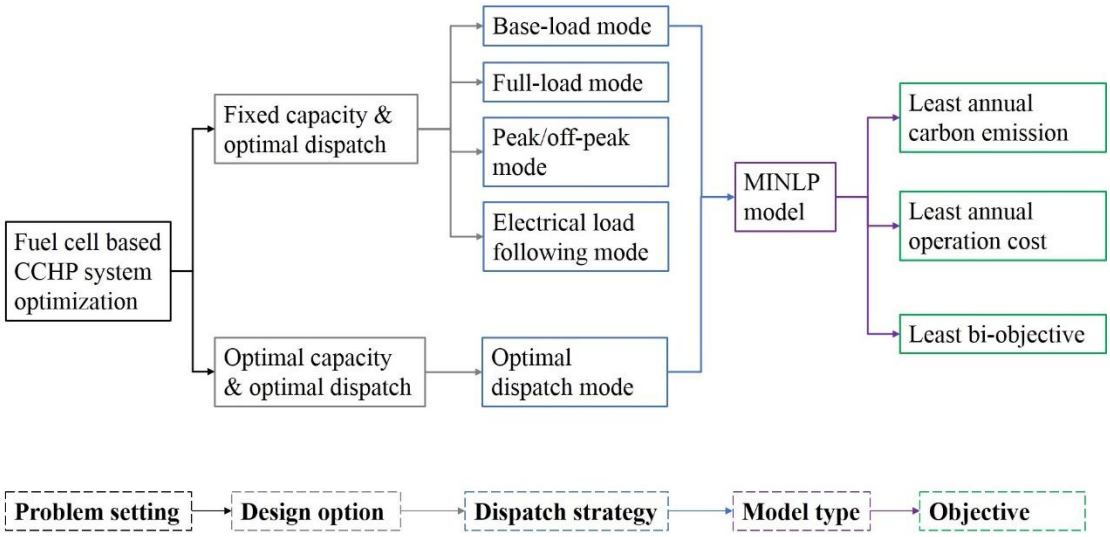

Fig. 2. Logic flow chart of the study.

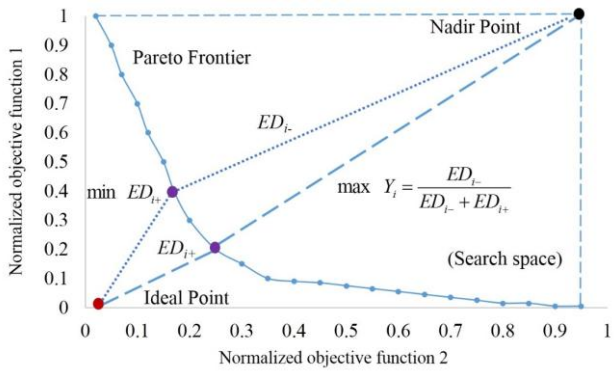

Fig. 3. Illustration of non-dominated and bi-objective decision making approaches.

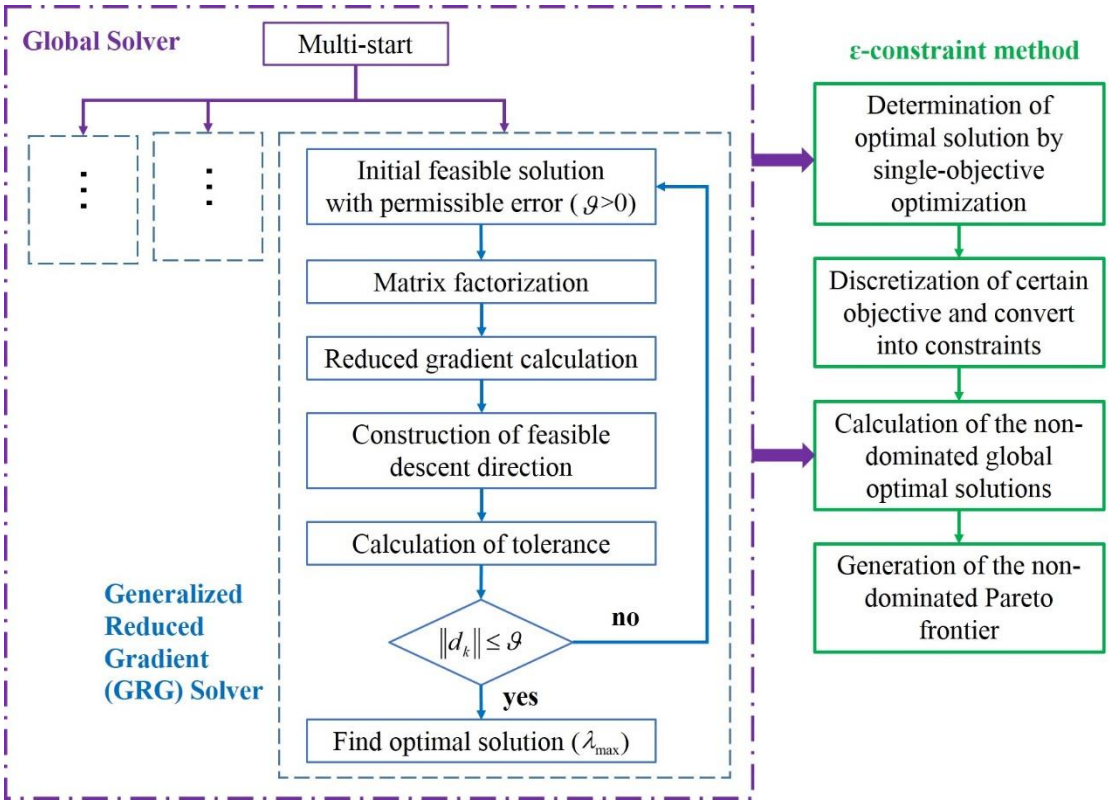

Fig. 4. Flow chart of multi-objective MINLP model solving procedure.

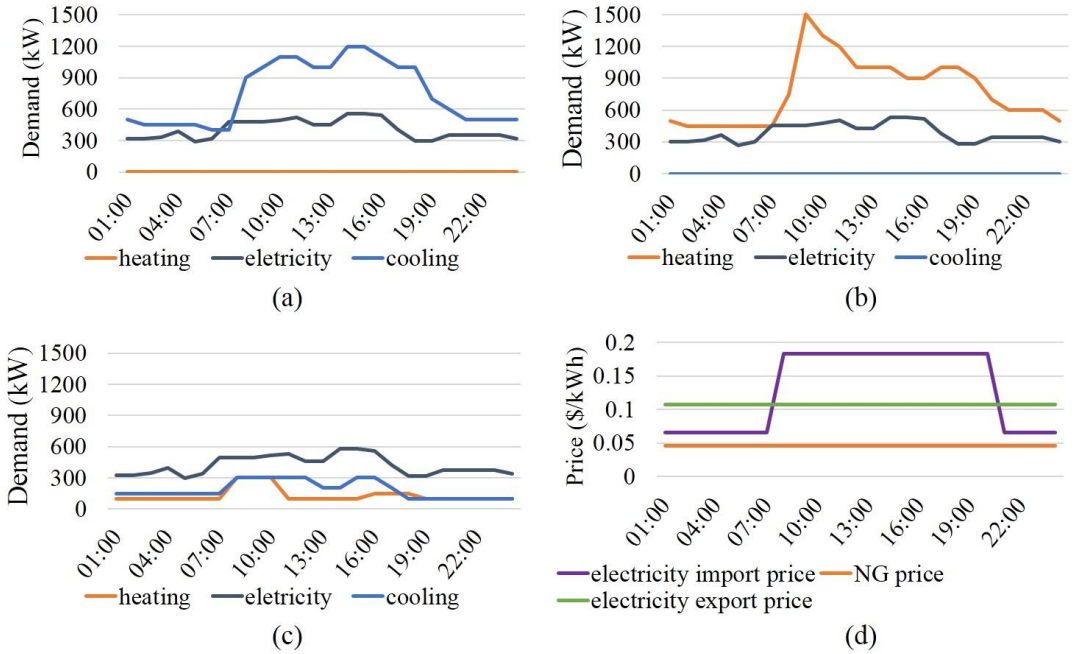

Fig. 5. Energy demand profiles of summer (a) winter (b) transition season (c) and energy prices (d).

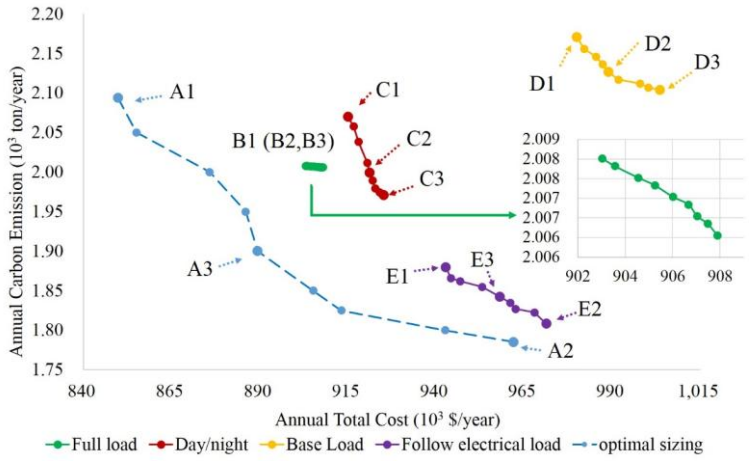

Fig. 6. Pareto frontiers for each sizing option and dispatch strategies.

Optimal sizing option		Fixed sizing option							
		Full load		Day/night		Base Load		Follow electrical load	
ED_{i+}	Y_i	ED_{i+}	Y_i	ED_{i+}	Y_i	ED_{i+}	Y_i	ED_{i+}	Y_i
1.000	0.500	1.000	0.500	1.000	0.500	1.000	0.500	1.000	0.500
0.859	0.529	0.907	0.497	0.894	0.489	0.784	0.545	0.882	0.510
0.733	0.530	0.812	0.474	0.741	0.513	0.673	0.559	0.782	0.511
0.624	0.568	0.794	0.449	0.680	0.523	0.576	0.599	0.747	0.493
0.513	0.637	0.792	0.444	0.671	0.548	0.510	0.640	0.694	0.520
0.536	0.636	0.850	0.433	0.712	0.550	0.537	0.639	0.741	0.493
0.579	0.627	0.861	0.472	0.767	0.551	0.770	0.543	0.740	0.515
0.829	0.538	0.930	0.479	0.883	0.524	0.859	0.529	0.903	0.471
1.000	0.500	1.000	0.500	1.000	0.500	1.000	0.500	1.000	0.500

Fig. 7. LINMAP and TOPSIS decision making details.

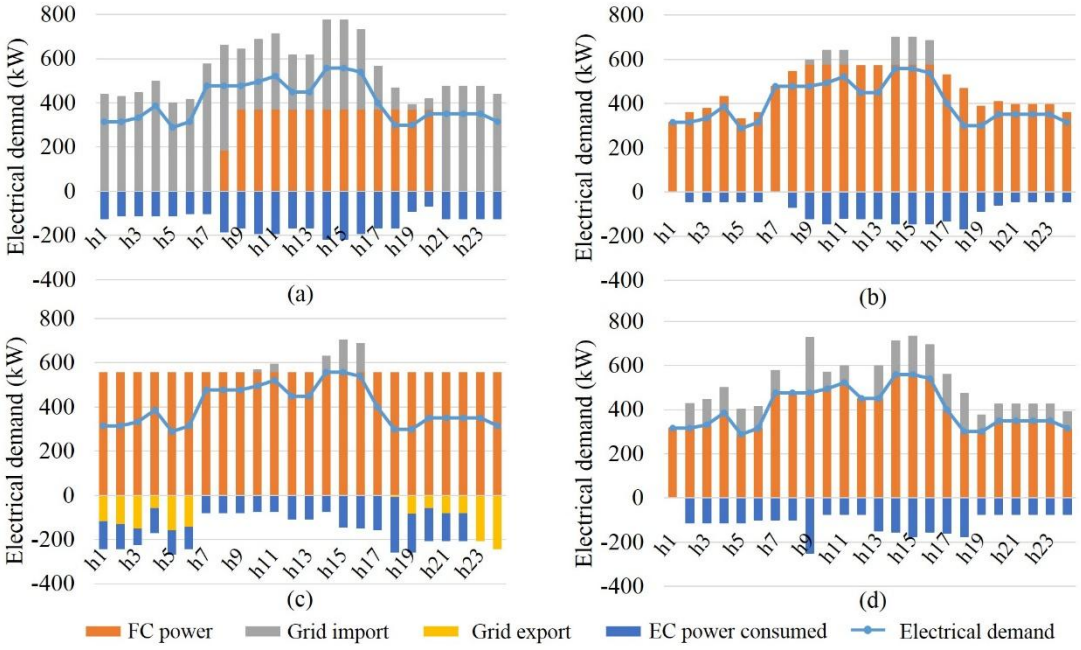

Fig. 8. Summer electrical balances of A1 (a) A2 (b) B (c) and E1 (d) optimal solutions (A1-optimal sizing with objective of the least ATC, A2-optimal sizing with objective of the least ACE, B-fixed sizing with full load operation mode, E1- fixed sizing with following electrical load operation mode).

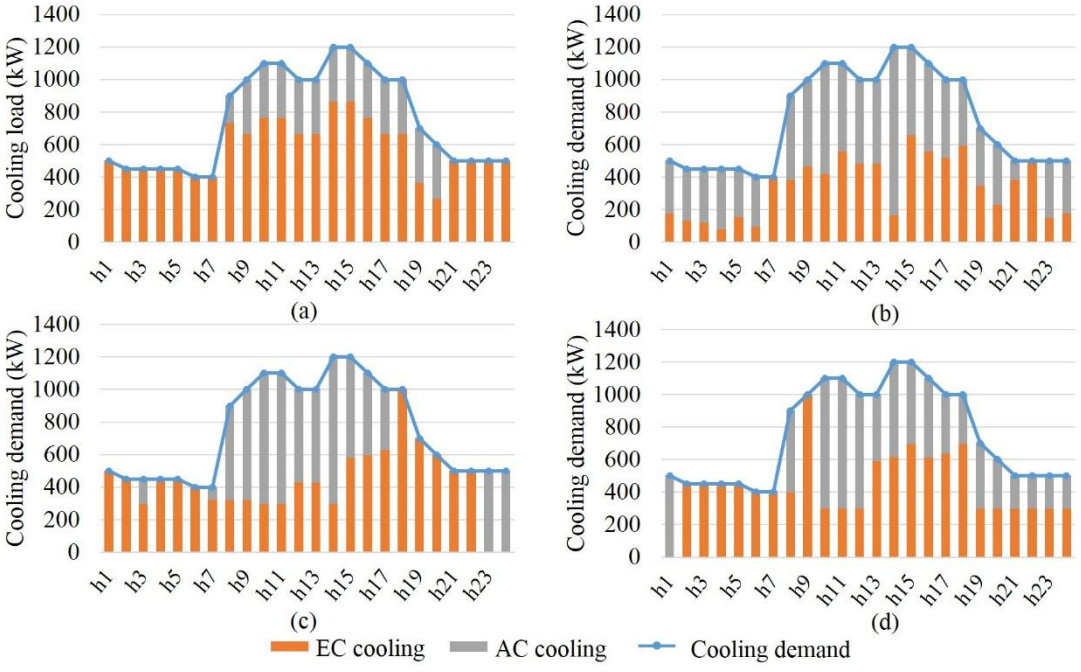

Fig. 9. Summer cooling balances of A1 (a) A2 (b) B (c) and E1 (d) optimal solutions.

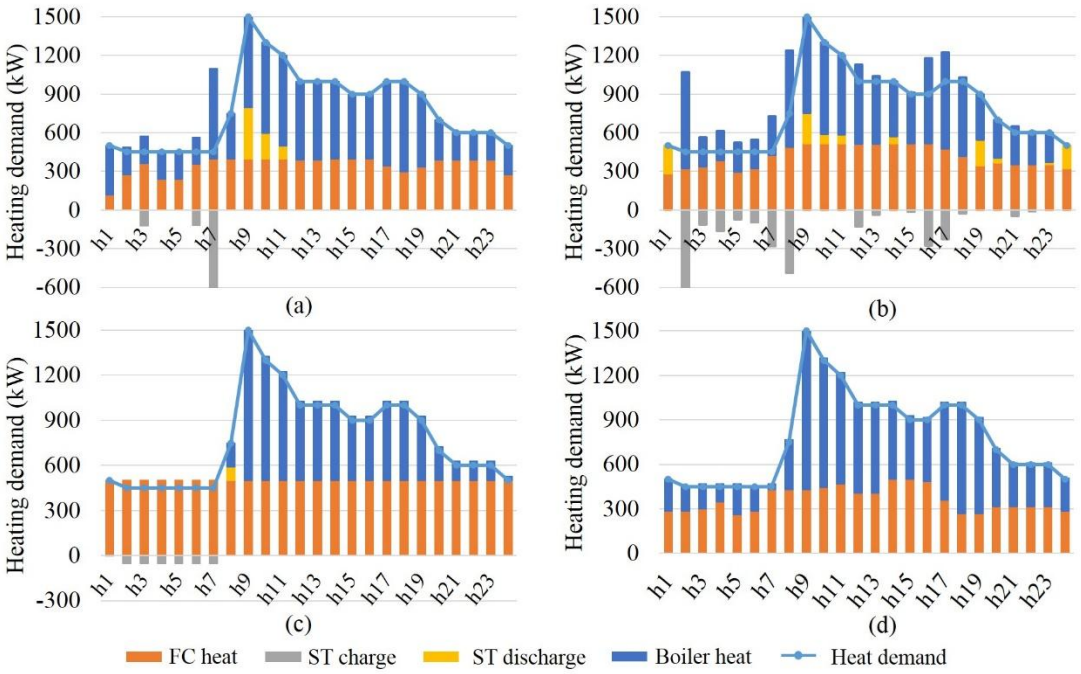

Fig. 10. Winter heating balances of A1 (a) A2 (b) B (c) and E1 (d) optimal solutions.

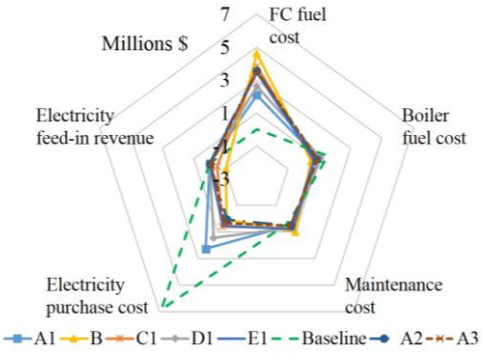

Fig. 11. Radar figure of OPEX breakdown comparison.

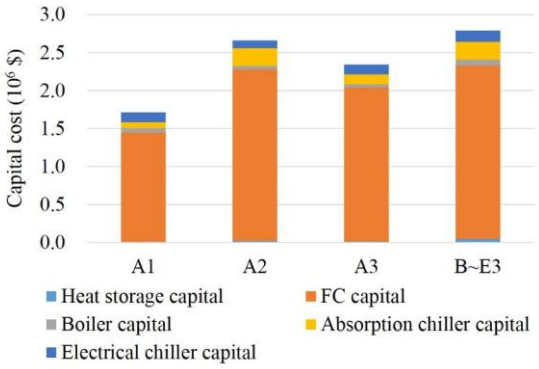

Fig. 12. Capital cost breakdown comparison.

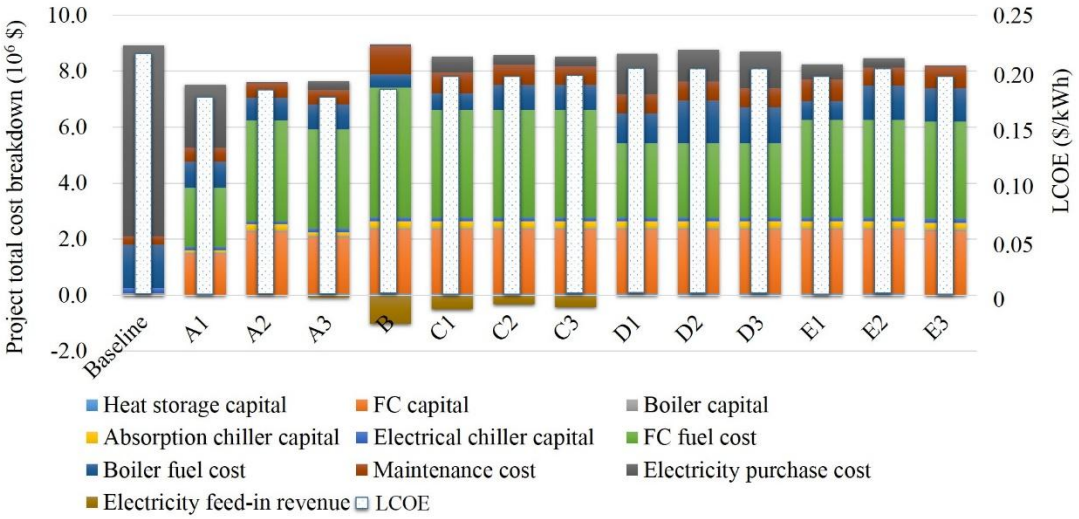

Fig. 13. Project total cost breakdown and LCOE comparison.

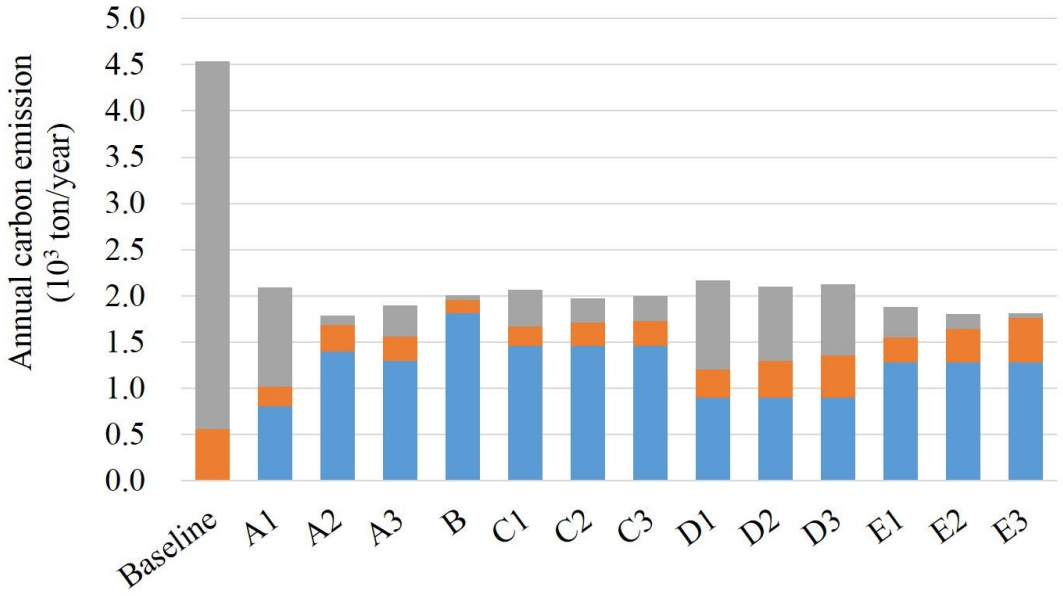

Fig. 14. Annual carbon emission comparison of each options.

Table 1. Project general information and emission factor. [3, 13, 14, 50]

Parameters	value	unit
Project lifetime	10	years
Interest rate	6	%
Natural gas emission factor (∂_{NG})	0.18	kg/kWh (LHV)
Grid electricity emission factor (∂_{grid})	0.95	kg/kWh

Table 2. Technical input parameters of major components. [3, 21, 23, 27, 37, 50]

System	Parameters	value	unit
SOFC	Design stack efficiency	58	%
	Design system efficiency (η_{fc})	45	%
	Daily start limit (φ)	1	
	Maximum capacity (CAP_{fc})	580	kW
	Stack lifespan	5	years
	Stack replacement	1,200	$/kW
Boiler	Design efficiency (η_b)	85	%
	Maximum capacity (CAP_b)	1,500	kW
Absorption chiller	Design efficiency (η_{ac})	1.1	
	Maximum capacity (CAP_{ac})	1,200	kW
Electrical chiller	Design efficiency (η_{ec})	4	
	Maximum capacity (CAP_{ec})	1,200	kW
Heat storage	Heat stored efficiency (η_{st})	95%	
	Heat charge efficiency ($\eta_{st\text{-}in}$)	95%	
	Heat discharge efficiency ($\eta_{st\text{-}out}$)	95%	
	Maximum capacity (CAP_{st})	2,000	kW

Table 3. Economic input parameters of major components. [3, 38, 53]

Device	Capital cost (C^{cap})	Maintenance cost (C^{maint})
	$/kW	$/kWh
SOFC	3,000	0.02
Boiler	50	0.0005
Absorption chiller	230	0.002
Electrical chiller	150	0.002
Heat storage	25	0.0005

Table 4. Baseline condition system capacity and performance.

Item	Component	value	unit
Installed capacity	Boiler	1,500	kW
	Electrical chiller	1,200	kW
Emission performance	Carbon emission	4,598	ton/year
Economic performance	Fuel cost	155,165	$/year
	Electricity cost	681,729	$/year
	Maintenance cost	29,099	$/year
	Annualized capital cost	34,654	$/year
	Levelized cost of energy*	0.20	$/kWh

* the energy refers to total energy, including electricity, heating and cooling.

Table 5. System design and performance comparison of each point.

Sizing and dispatch strategy		Point	Installed capacity					Grid electricity		System performance	
			FC (kW)	Boiler (kW)	Electrical chiller (kW)	Absorption chiller (kW)	Heat storage (kW)	Export (kWh/year)	Import (10^3 kWh/year)	ACE (ton/year)	ATC (10^3 $/year)
Optimal sizing and dispatch		A1	370	1,111	866	333	246	-	1,826	2,094	849
		A2	578	900	660	1,033	913	-	75	1,785	962
		A3	512	1,000	740	470	520	77	198	1,900	889
Fixed sizing	Full load	B	578	1,500	1,000	1,000	2,000	937	64	2,007	906
	Day/night	C1						481	321	2,070	915
		C2						321	297	1,971	925
		C3						388	285	1,999	921
	Base load	D1						-	1,100	2,171	980
		D2						-	839	2,104	1,003
		D3						-	992	2,127	990
	Following electrical load	E1						-	350	1,880	943
		E2						-	190	1,808	971
		E3						-	45	1,842	958